https://doi.org/10.5194/egusphere-2025-1483
Preprint. Discussion started: 3 June 2025

Machine learning significantly improves the simulation of hourly-to-yearly scale cloud nuclei concentration and radiative forcing in polluted atmosphere

Jingye Ren[1,2], Songjian Zou[3], Honghao Xu[3], Guiquan Liu[3], Zhe Wang[3], Anran Zhang[3], Chuanfeng Zhao[4], Min Hu[5], Dongjie Shang[5], Lizi Tang[5], Ru-Jin Huang[1], Yele Sun[6], Fang Zhang[3]*

[1]State Key Laboratory of Loess Science, Institute of Earth Environment, Chinese Academy of Sciences, Xi'an, 710061, China

[2]Xi'an Institute for Innovative Earth Environment Research, Xi'an, 710061, China

[3]School of Civil and Environmental Engineering, Harbin Institute of Technology, Shenzhen, 518005, China

[4]Department of Atmospheric and Oceanic Sciences, School of Physics, Peking University, Beijing, 100871, China

[5]State Key Joint Laboratory of Environmental Simulation and Pollution Control, College of Environmental Sciences and Engineering, Peking University, Beijing, 100871, China

[6]State Key Laboratory of Atmospheric Boundary Layer Physics and Atmospheric Chemistry, Institute of Atmospheric Physics, Chinese Academy of Sciences, Beijing, 100029, China

Corresponding author: Fang Zhang, *zhangfang2021@hit.edu.cn*

https://doi.org/10.5194/egusphere-2025-1483
Preprint. Discussion started: 3 June 2025

Abstract

The accurate prediction of cloud condensation nuclei (CCN) number concentration (N_{CCN}) on a large spatiotemporal scale is challenging but critical to evaluate the aerosol cloud interaction (ACI) effect. Combining multi-source dataset and the N_{CCN} simulated by the Weather Research and Forecasting coupled with Chemistry (WRF-Chem) model, we have developed a new machine learning-based model which predicts well both regional and hourly-to-yearly scale N_{CCN} at typical supersaturations in the North China Plain (NCP). We show that the prediction bias of N_{CCN} compared to observations is reduced from -39% with the WRF-Chem model to approximately -8% with the new model. The greatest improvement is seen in polluted cases. The new model captures well the spatial variation and better describes long-term trends of N_{CCN} than the WRF-Chem. More importantly, the study reveals a significant long-term decreasing trend of N_{CCN} in NCP due to a rapid reduction in aerosol concentrations from 2014 to 2018, during which a series of strict emission reduction measures were implemented by the Chinese government. This reflects the climate benefit of pollution control. Our study further illustrates that the new model reduces the uncertainty in simulating cloud radiative forcing from an overestimation of 1.07±0.76 W m^{-2} to only 0.18±0.65 W m^{-2}, illustrating the high sensitivity of climate forcing to changes in N_{CCN}. This work offers a new modeling framework that has the potential to greatly improve the assessment of the ACI effect in current models, and guides the way to simulate CCN in other regions around the world.

https://doi.org/10.5194/egusphere-2025-1483
Preprint. Discussion started: 3 June 2025

1. Introduction

Aerosol indirect radiative effects caused by aerosol-cloud interactions (ACI) are the largest source of uncertainty when assessing climate change (IPCC 2021). A major issue is the lack of an accurate characterization of cloud condensation nuclei (CCN, or cloud nuclei) number concentrations (N_{CCN}) in global climate models (Sotiropoulou et al., 2007; Fanourgakis et al., 2019). This is largely due to the nonlinear interactions between the aerosol physical and chemical properties and CCN, making the quantification of the N_{CCN} remain highly uncertain. Current models tend to underestimate CCN number concentrations by 20–40% on average, based on comparisons between results from 14 models and observations at sites distributed globally (Fanourgakis et al., 2019). Biases were greater in the Northern Hemisphere due to intensive human activities (Sotiropoulou et al., 2007). It has been proposed that ~10–30% changes in cloud droplet concentrations might be associated with the uncertainties in cloud radiative forcing by ~0.1–2 W m^{-2} (Charlson et al., 1987; Sotiropoulou et al., 2007; Yu et al., 2022). Towards improving estimates of the ACI effect in modeling, it is critical to obtain accurate spatiotemporal distributions of CCN.

Predicting N_{CCN} remains challenging because aerosol CCN activity varies greatly in time and space and involves microphysical and chemical processes. Previous studies have underscored that the main uncertainties in simulating N_{CCN} at regional and global scales are the simplified representations of particle size distribution (Menon & Rotstayn, 2006), as well as the lack of detailed treatment of the microphysical and chemical

https://doi.org/10.5194/egusphere-2025-1483
Preprint. Discussion started: 3 June 2025

processes in current models (Sha et al., 2019; Yu et al., 2020). Therefore, a considerable number of CCN closure studies have been carried out to predict N_{CCN} in different environments (Moore et al., 2012; Zhang et al., 2014, 2016, 2017, 2019; Xu et al., 2021; Ren et al., 2018, 2023). Although extensive CCN observations and closure studies might help to reconcile this uncertainty, field measurements are relatively sparse and have only been collected during a few campaigns at a few sites (Schmale et al., 2018; Rose et al., 2021) due to the limitations of techniques and cost. Closure studies, however, have mostly focused on investigating the relative importance of the aerosol physical and chemical properties to CCN prediction and have not yet provided a CCN parameterization scheme that is applicable to different regions over the globe. Some studies have attempted to develop a correlation between aerosol optical properties and CCN number concentrations (Rosenfeld et al., 2016). Compared with the measurement of CCN at ground sites, satellite retrieval methods offer global coverage with high spatial and temporal resolutions (Rosenfeld et al., 2016; Liu et al., 2020). However, they are limited to clear-sky conditions. Due to the aerosol swelling effect (Liu et al., 2018), there are typically large deviations of -30% to +90% in the estimation accuracy of N_{CCN} in different environments (Shen et al., 2019).

In recent years, machine learning (ML) has been used for the inversion of atmospheric environmental parameters such as tropospheric ozone and particulate matter with a diameter of 2.5 μm or smaller ($PM_{2.5}$) (Grange et al., 2018; Geng et al., 2021; Wei et al., 2023). To our knowledge, ML-based prediction of CCN properties is few and far between, with studies only focused on analyzing the importance of different

https://doi.org/10.5194/egusphere-2025-1483
Preprint. Discussion started: 3 June 2025

variables to estimating CCN spectra at a single field site (Liang et al., 2022) or were conducted in relative clean regions (Nair et al., 2020, 2021). It would be a step forward to use an ML-based method to predict N_{CCN} in polluted areas because it would help to verify the applicability of the method in different regions, but most importantly, it would improve model simulations of the ACI effect in polluted regions where errors in predicting N_{CCN} are greater than in clean regions.

In this study, we have developed a new ML-based model for predicting N_{CCN} on hourly-to-yearly scale in the heavily polluted North China Plain (NCP) by using a multi-source dataset of atmospheric variables and CCN concentration outputs from the Weather Research and Forecasting coupled with online chemistry (WRF-Chem) model. The diagram of the model construction and the N_{CCN} prediction is shown in Figure 1. We have presented and analyzed the relative importance of the different parameters to CCN prediction; Moreover, we have verified the performance of the new model in predicting the N_{CCN} over different temporal and spatial scales in the NCP. Finally, by incorporating the N_{CCN} prediction biases into the evaluation of cloud parameters and radiative forcing, we investigate the sensitivity of aerosols indirect climate forcing to CCN concentrations changes.

2. Data collection and model construction

In this study, we develop the ML-based model by employing the Random Forest Regression method (RFRM) and outputs of N_{CCN} from the WRF-Chem model. A region within 32°-40°N and 114°-121°E in the NCP is chosen as the study area (Fig. S1 and

https://doi.org/10.5194/egusphere-2025-1483
Preprint. Discussion started: 3 June 2025

Section 1 in the online supplemental Information SI). In the WRF-Chem modeling system, the sectional Model for Simulating Aerosol Interactions and Chemistry (MOSAIC) is used here (see Section 2 in the SI). The simulation in WRF-Chem is conducted from 1 January 2014 to 31 December 2018 with an hourly resolution. The Morrison two-moment scheme (Morrison et al., 2009) and the Carbon Bond Mechanism Z photochemical mechanism (Zaveri et al., 1999) are employed in the WRF-Chem model. SI gives more details about the other parameterizations used. The simulated N_{CCN} is as one of the input parameters of the RFRM model which has been trained and validated with field observational dataset obtained at the sites in this region.

Other input parameters include the chemical components of $PM_{2.5}$ from the Tsinghua University Tracking Air Pollution in China dataset (Geng et al., 2021) and gas and particulate pollutants (nitrogen dioxide (NO_2), sulfur dioxide (SO_2), carbon monoxide (CO), ozone (O_3) and $PM_{2.5}$) collected from the China National Environmental Monitoring Centre network. Meteorological parameters are from the European Centre for Medium-range Weather Forecasts Reanalysis version 5 (ERA-5) and include temperature, relative humidity (RH), total precipitation (TP), wind speed (WS), wind direction (WD), planetary boundary layer height (BLH), surface pressure (SP) and surface net solar radiation (SNSR). Cartesian coordinates were also added as input due to the spatiotemporal nature of the input data (Yang et al., 2022). Table S1 and Section 3 of SI provide more details about the input parameters. Cross-validation (Nair et al., 2020) is also applied to select the hyperparameters during the data preprocessing (Fig. S2).

https://doi.org/10.5194/egusphere-2025-1483
Preprint. Discussion started: 3 June 2025

Ground measurements of atmospheric gaseous precursors, fine particles chemical compositions, and CCN number concentration (at supersaturations of 0.2% and 0.4%) were collected during six field campaigns at three sites in the NCP (Fig. 3), used to assess the performance of the developed ML-based model in predicting N_{CCN}. More details about the ground-based N_{CCN} measurements and instrumentation can be found in Section 5 of SI.

3. Results

3.1 The relative importance of the input parameters to the prediction of N_{CCN}

The relative importance of the input parameters in predicting N_{CCN} is quantified in Fig. 2. The permutation score of the importance of each individual parameter is calculated by randomly permuting values of the parameters and establishing the association with RFRM-predicted N_{CCN}. Nitrate (NO_3^-) emerges as the most crucial indicator with the highest permutation score (~0.48–0.74) and correlation (~0.54). This is likely due to the increment increase in the proportion of nitrate aerosols in $PM_{2.5}$ in recent years (Li et al., 2020; Liang et al., 2022), which are highly hygroscopic, so dominates changes in particle hygroscopicity and CCN activity. The important role of NO_3^- can also be indicated by the good consistency of temporal variations of the field measured NO_3^- and N_{CCN} (Fig. S3).

The importance of $PM_{2.5}$ mass concentration, which is associated with the changes in particle size and composition (Zhang et al., 2019), is secondary to NO_3^- particles in the summer seasons, normally an increase of $PM_{2.5}$ corresponding to enhanced CCN

https://doi.org/10.5194/egusphere-2025-1483
Preprint. Discussion started: 3 June 2025

activity. During the winter, changes in BLH contribute more to CCN predictions than $PM_{2.5}$ (Fig. 2b) and more to the model's output (Fig. 2c). This is a season when the planetary boundary layer strongly influences the evolution of haze and the accumulation of particles in the lower atmosphere. Such effects are not as important in summer (Zhang et al., 2019; Song et al., 2022). As reported in Guo et al. (2016), the BLH would decrease significantly with the increase of the aerosol mass concentration. Clearly, CCN predictions highly depend on the time and seasons. In addition, compared to winter, the black carbon (BC) mass concentration plays a more important role in the summer half year when the rapid aging processes of BC occurred and thus enhanced the CCN activity (Ren et al., 2023). Note that the impact of sulfate aerosols on N_{CCN} prediction is much less important in both summer and winter seasons compared to nitrate particles, with a permutation score ranging from ~0.02 to 0.03, largely due to its decreased proportion in $PM_{2.5}$ in recent years (Liang et al., 2022; Li et al., 2020).

The results also show the important role of the ambient temperature in the winter half year, which is mainly reflected in the promotion of nucleation growth and secondary generation of particles (Song et al., 2022). While in the summer half year, the RH has a higher importance score in N_{CCN} prediction, which is conducive to the hygroscopic activation of particles (Chen et al., 2022). By comparison, the permutation score of other meteorological factors (eg., WS, WD, TP, SP and SNSR) are relatively low (< 0.06) both in summer and winter half year in the NCP.

In addition, among the gaseous pollutants, the NO_2 is found to be the most important factor when predicting N_{CCN}, which may be due to the production of nitrate

https://doi.org/10.5194/egusphere-2025-1483
Preprint. Discussion started: 3 June 2025

(Li et al., 2020). However, different from previous reports by Nair and Yu (2020), other gas precursors are less important with low permutation score values. In summary, the critical important parameters for predicting N_{CCN} include the $PM_{2.5}$, chemical components (nitrate, organics and BC), meteorological factors (RH, BLH, and TEM), and gaseous precursors (NO_2). However, the importance of each input parameters in predicting CCN varies with time such as seasons.

3.2 Performance of the new model in predicting N_{CCN} at field sites in the NCP

To examine the performance of the newly developed model in predicting N_{CCN}, we compare the predicted N_{CCN} with both the simulations by WRF-Chem and the observations from six field campaigns in NCP (Fig. 3). The six campaigns, named as BJ2014_WIN, BJ2015_AUT, BJ2016_WIN, BJ2017_SUM, XT2016_SUM, and GC2018_WIN, were conducted in different seasons at three sites in the NCP (Fig. 3a). The observed N_{CCN} varies from a few hundred to tens of thousands at these sites, and the campaign mean mass concentration of $PM_{2.5}$ ranges from 35.6 to 160 μg m^{-3} (Fig. 3b), indicating that the observations can represent various atmospheric conditions, spanning from clean to polluted in the region. Fig. 3a shows N_{CCN} at a supersaturation of 0.2% (the typical range of supersaturations in clouds). It shows that, for all the six campaigns, the time series of N_{CCN} predicted by the new model agrees better with the observed N_{CCN} compared to simulations by the WRF-Chem model. Although both the new model and WRF-Chem exhibit underestimations in observed N_{CCN}, the average bias between the predicted and observed N_{CCN} has been reduced from -39% by the WRF-Chem model to approximately -8% by the newly constructed model (Fig. 3c).

https://doi.org/10.5194/egusphere-2025-1483
Preprint. Discussion started: 3 June 2025

Compared to WRF-Chem simulations, the new model showed the greatest improvement during the winter campaigns when $PM_{2.5}$ concentrations were usually higher. For example, during the GC2018_WIN campaign, the observed N_{CCN} is underestimated as large as 61% by the WRF-Chem (Fig. S4), while the underestimation is largely improved with the predicted bias of only 3% in the new model (Fig. S4). WRF-Chem simulations for warm seasons noticeably improved, e.g., the uncertainty decreased to 8% during the BJ2015_AUT campaign (Fig. S4). Overall, the new model still performs better than the WRF-Chem model and is with averaged predicted bias of 18% during summer campaigns. Occasionally, the WRF-Chem model overestimated the N_{CCN} apparently, e.g., the episodes of September 21 to 24 during the BJ2015_AUT campaign, and May 28 to 31 during the BJ2017_SUM campaign. Figure S5 shows comparisons of N_{CCN} at S=0.4%, which exhibits similar patterns to that at S=0.2%. Overall, the new model performs well and can accurately capture the observed fluctuations during these episodes. The improvements in our new model also demonstrate the effectiveness of the model trained on data on a daily scale to data on an hourly scale.

The large biases of the WRF-Chem to simulate N_{CCN} may be caused by the uncertainties in precursor vapor mass, size distributions of the particles, the hygroscopic properties of the organics, dry deposition and cloud processing, which have been noted and proposed by Fanourgakis et al. (2019). In our case, the underestimation of N_{CCN} by the WRF-Chem model is likely due to the overestimation of the organics and BC mass fraction induced by WRF-Chem (Fig. S6), the simplified

https://doi.org/10.5194/egusphere-2025-1483
Preprint. Discussion started: 3 June 2025

prescriptions in particle size distribution, and the bias of the hygroscopic parameter of organics. Also, the fixed hygroscopicity parameter value does not sufficiently represent the hygroscopicity of organics throughout the study period (Liu et al., 2021). Note that for the periods of November 16 to 21 during the BJ2016_WIN campaign, N_{CCN} is considerably overpredicted by the new model. This may be due to the extremely high levels of primary organic aerosol (POA) during that period (Fig. S7), resulting in weakened aerosol hygroscopicity and CCN activity, thereby lowering CCN number concentrations (Fan et al., 2020). Neglecting to distinguish between POA and SOA information during the training of the new model may cause the overestimation of N_{CCN} when POA dominates. Uncertainties incurred by the new model could also originate from the lack of physical interpretability in these ML-based models (Wei et al., 2023). Additional input parameters that carry rich and meaningful information (e.g., size distribution, aerosol sources and other secondary processes) are expected to further improve the predictability of N_{CCN} in future.

3.3 Performance of the new model in predicting hourly-to-yearly-scale N_{CCN}

To further examine the performance of the new model in predicting N_{CCN} at different time scales, we compare the new model-predicted hourly-to-yearly N_{CCN} in Beijing with both WRF-Chem simulations and observed values (Fig. 4). The new model captures well the diurnal cycle (Fig. 4a), while the WRF-Chem model underestimates N_{CCN}, especially at night. Concerning seasonal variations, similarly, the new model performs better with the mean bias of ~ 6% compared to observations. While the mean bias can increase to be ~25% by the WRF-Chem (Fig. 4b). Note that, the bias is much

https://doi.org/10.5194/egusphere-2025-1483
Preprint. Discussion started: 3 June 2025

greater in the cold seasons than that in the warm seasons for the WRF-Chem. This is probably due to the higher wintertime CN and CCN concentrations which are more difficult for models to capture and simulate (Fanourgakis et al., 2019).

Figure 4c shows the long-term trend of yearly averaged N_{CCN}. Here, the real atmospheric long-term trend of N_{CCN} (denoted as N_{CCN_Obs}) is derived using the long-term measurement of particle number size distribution (PNSD) at a field site in Beijing (Fig. S8) (Fig. 4d, Shang et al., 2022) and the κ calculated from the measured chemical compositions based on the κ-Köhler theory (Petters and Kreidenweis, 2007). The results show that the predicted average annual N_{CCN} at S=0.2% based on the new model agrees well with N_{CCN_Obs} in terms of magnitude and long-term trend (Fig. 4c), showing a decreasing trend year by year with the average annual CCN number concentration of about 6216±3624 cm^{-3} in 2014 and 3278±2306 cm^{-3} in 2018; however, although the WRF-Chem simulations also show a similar decreasing trend year by year, it significantly underestimates the average annual N_{CCN} of all years (with average bias of 43%), resulting in the inter-annual trend lines being parallel but not coincident. The small bias (within ±5%) between the new model predictions and the observations may be due to the uncertainty from how N_{CCN_Obs} is calculated , i.e., using the Tracking Air Pollution in China (TAP) dataset to calculate κ. A comparison of the values of κ and N_{CCN} between that derived using field observations and the TAP dataset shows little differences (Fig. S9); actually, the long-term change of N_{CCN} is much less sensitive to changes in κ values compared to the PNSD, and thus the uncertainty in the long-term N_{CCN_Obs} caused by using the TAP dataset is negligible (Fig. S9). The method to

https://doi.org/10.5194/egusphere-2025-1483
Preprint. Discussion started: 3 June 2025

calculate N_{CCN} at S=0.2% based on κ-Köhler theory would cause an upper-limit uncertainty of 7% (Ren et al., 2018).

According to Fig. 4d-e, the long-term decreasing trend of N_{CCN} at S=0.2% from 2014 to 2018 is mainly attributed to a significant reduction in aerosol particle number concentrations in the atmosphere. In addition, the peak diameter of the PNSD shows a shift toward the left, decreasing slightly from about 70 nm in 2014 to 30 nm in 2018 due to the enhanced new particle formation events in recent years (Zhu et al., 2021). This would also result in less aerosol particles serving as CCN. Although the κ_{chem} has a slight upward trend from 2014 to 2018 (Fig. 4e), yielding decreases in activation diameter and thereby more CCN, the aerosol particle hygroscopicity, however, plays much less significant role in regulating the total N_{CCN} compared to the changes in particle number size distribution during this period.

3.4 Spatial variations of N_{CCN} derived by the new model and WRF-Chem

We further examine the spatiotemporal changes of N_{CCN} at S=0.2% in the NCP derived by the new model and WRF-Chem (Fig. 5). Regionally, the N_{CCN} predicted by the new model is also generally higher than that simulated by WRF-Chem at most of the sites. The N_{CCN} derived by the new model and WRF-Chem both decrease from 2014 to 2018 but with different decreasing rates (Fig. 5c-e). On average, N_{CCN} derived by the new model and WRF-Chem decrease from 4996±1147 to 3930±884 cm^{-3} and from 2834±1366 to 2111±546 cm^{-3} respectively from 2014 to 2018 in the NCP region (Fig. 5c), corresponding to annual decreasing rates of approximately ~ -247 cm^{-3} yr^{-1} (-4% yr^{-1}) for the new model and ~ -167 cm^{-3} yr^{-1} (-5% yr^{-1}) for the WRF-Chem model (Fig.

https://doi.org/10.5194/egusphere-2025-1483
Preprint. Discussion started: 3 June 2025

5d-e). Moreover, N_{CCN} and its changes from 2014 to 2018 predicted by the new model show more significant spatial variations than that simulated by the WRF-Chem model. Differences in new-model-predicted N_{CCN} between 2014 and 2018 (2018 minus 2014) show negative values at ~90% of the sites, i.e., downward trends in N_{CCN} (Fig. 5c1). The sites with apparent N_{CCN} reduction are mainly located in the central and northern of NCP, especially in Beijing-Tianjin-Hebei (BTH) and central Shandong, where are mostly impacted by heavy industry and densely populated (Wei et al., 2023). Sites in southern NCP have slight downward trends in N_{CCN}. The downward trend is consistent with the variations in concentration of gaseous pollutants due to the emission reduction in past years in China (Fig. S10). Interestingly, note a few sites with positive values (upward trends in N_{CCN}) are mainly located along the coast. An increase in the fraction of accumulation-mode particles in coastal areas has been reported contributing more CCN (Zhu et al., 2021). This demonstrates the good performance of the new model in capturing the real-time spatial variations of CCN on a regional scale. By contrast, WRF-Chem simulation fails to capture such spatial variations, showing overall decreasing trends at all sites in the NCP (Fig. 5c-e).

In summary, our newly constructed model can capture the spatial variability in the long-term trend of N_{CCN}, while the WRF-Chem model might mask the variations of N_{CCN} among different sites. This will smooth out the true impact of aerosols on weather and climate at regional or local scales, leading to uncertainties in model simulations.

https://doi.org/10.5194/egusphere-2025-1483
Preprint. Discussion started: 3 June 2025

3.5 Sensitivity of the cloud parameters and radiative forcing to CCN prediction biases

To evaluate the effects introduced by N_{CCN} prediction biases to the aerosol indirect effects, we further incorporate the deviations between observed N_{CCN} (denoted as CCN_{OBS}) and N_{CCN} predicted by the new model (denoted as CCN_{ML}) and the simulated by the WRF-Chem model (denoted as $CCN_{WRF\text{-}Chem}$) into calculations of the cloud parameters and radiative forcing, as are shown in Fig. 6 (for S =0.2%) and Figs. S11-13 (for S=0.1%, and 0.4%). Typically, aerosol particles serving as CCN could indirectly affect the global climate by the Twomey (Twomey, 1977) and Albrecht effects (Albrecht, 1989). According to Wang et al. (2019), two parameters of cloud optical thickness (τ) and the absorption coefficient (1-ω_0) can be used to estimate the Twomey effects. The process of cloud-to-rain conversion, which can be parameterized by the critical radius (r_c) and the cloud-to-rain conversion threshold function (TA), is critical to estimate the Albrecht effect. Therefore, the r_c and TA is also calculated here. Indirect (cloud) radiative forcing (F_c) is also evaluated based on the deviations in CCN number concentration under the assumption of a constant liquid water content (Charlson, 1992; Wang et al., 2008). Section 6 of the SI provides details about the methods used to evaluate aerosol indirect effects.

In general, the results show that these cloud properties are more sensitive to the changes in N_{CCN} when the models underestimate the CCN number concentrations (ΔN_{CCN}<0) compared to the cases with an overestimation (Figure. 6a-d). For example, a ~50% underestimation (overestimation) of N_{CCN} could lead to relative deviations

https://doi.org/10.5194/egusphere-2025-1483
Preprint. Discussion started: 3 June 2025

(uncertainties) of -21% (14%) for τ, 27% (-12%) for (1-ω_0), and -11% (7%) for r_c at S=0.2%. Note that, on average, both the new model and WRF-Chem in this study show underestimations in N_{CCN} within the sensitivity zone of the cloud effect (Fig. 6), It is thus expected to cause large uncertainties in evaluating the cloud radiative forcing, a topic worthy of further attention. Given that the uncertainty in N_{CCN} predicted by the WRF-Chem model is much greater than that of our new model, the uncertainties and variation ranges of these cloud parameters from WRF-Chem simulations are also greater. Specifically, the uncertainties of CCN_{ML} and $CCN_{WRF\text{-}Chem}$ lead to the uncertainties of -52% to +91% and -77% to +171% respectively, for the τ (Fig. 6a and a1), -47% to +112% and -63% to +344% respectively, for the 1-ω_0 (Fig. 6b and b1), -31% to +38% and -53% to +65% respectively, for the r_c (Fig. 6c and c1), and -256% to +210% and -434% to +353% respectively, for the TA (Fig. 6d and d1).

In addition, the underestimation of CCN would lead to underestimations of cloud optical thickness τ and the critical radius r_c of the automatic cloud/rain transformation, but overestimations of (1-ω_0) and the threshold function TA of the automatic cloud/rain transformation, all of which depend on their physical mechanisms within the realm of aerosol-cloud interactions (Stier et al., 2024) (Fig. S11). This is also the case at the other supersaturation levels considered (Fig. S11-S13).

As a result, we derive that the mean underestimation of ~39±80% in N_{CCN} at S=0.2% caused by the WRF-Chem leads to underestimations of 15±22% in the τ, 8±10% in the r_c, and an overestimation of 18±21% in the absorption coefficient (1-ω_0) and 53±73% in the TA. While, the uncertainties for all these parameters are largely reduced when the

https://doi.org/10.5194/egusphere-2025-1483
Preprint. Discussion started: 3 June 2025

mean underestimation of ~8±38% in N_{CCN} at S=0.2% that is caused by our new model is applied (Fig. 6e). For example, the underestimation of cloud optical thickness τ decreases to ~3%, an improvement compared to the underestimation of about 15% by the WRF-Chem model. Also, the new model reduces the underestimation of the critical radius r_c of the automatic cloud/rain transformation to only ~1%. Ultimately, the uncertainty of cloud radiative forcing F_c has been significantly reduced from an overestimation of 1.07±0.76 W m^{-2} by the WRF-Chem model to only 0.18±0.65 W m^{-2} by the new model, showing the high sensitivity of climate forcing to the uncertainties in CCN number concentrations. Note that a limitation when evaluating the cloud radiative forcing based on the assumption of cloud fraction and the fractional transmission is the approximate analytical expression. Therefore, the results presented here may represent the upper limit, and the sensitivity of the radiative forcing to changes in N_{CCN} would be weaker over continental areas (Wang et al., 2008; Yu et al., 2022).

4. Discussion and conclusions

In this study, using a multisource dataset of atmospheric variables and the N_{CCN} simulations by the WRF-Chem model, we have developed a new machine-learning-based model that predicts well prediction of regional-scale N_{CCN} based on the application of the model to data from the densely populated NCP region. The results show that the prediction bias of N_{CCN} compared to observations is reduced from -39% from WRF-Chem simulations to approximately -8% from the newly constructed model. The improvement is greatest during heavy pollution periods or cold seasons. In general,

https://doi.org/10.5194/egusphere-2025-1483
Preprint. Discussion started: 3 June 2025

our new model captures the spatial differences in N_{CCN} in the NCP better than the WRF-Chem model. In addition, the new model reveals a long-term downward trend of N_{CCN} coincident with the observed trend for the period of 2014–2018. By further incorporating the N_{CCN} prediction biases into the evaluation of cloud parameters and radiative forcing, we found that the cloud properties are more sensitive to the changes in N_{CCN} when the models underestimated the CCN number concentrations compared to the cases when the models overestimated N_{CCN}. As a result, the simulated uncertainty of cloud radiative forcing F_c could be significantly reduced from an overestimation of 1.07±0.76 W m^{-2} to only 0.18±0.65 W m^{-2} by the new model. Given the simplified setting in current climate models, this work emphasizes the necessity and urgency to obtain the precise N_{CCN} values, offering a new framework for predicting CCN concentrations based on machine learning algorithms. Incorporating this framework into traditional three-dimensional numerical or global climate models could help reduce the uncertainty of simulated aerosol indirect effects.

Note that in this study, observational data from six campaigns at three sites are analyzed. Validating the simulated N_{CCN} through comparisons with observations at more ground sites is thus warranted. In the future, it is crucial to obtain comprehensive monitoring data of CCN and other key aerosol properties (e.g., particle size distribution, chemical compositions) in different environments. Our modeling framework could then be used to simulate ground-level CCN data in other regions around the world and even on a global scale. This new modeling framework could also guide the way to developing

https://doi.org/10.5194/egusphere-2025-1483
Preprint. Discussion started: 3 June 2025

a new machine-learning-based model to predict CCN vertical profiles, which is useful for the accurate evaluation of the ACI effect.

Code and Data availability

The data and code are publicly accessible at https://zenodo.org/records/15523200 (Ren et al., 2025). This includes the machine learning code, the corresponding training and testing dataset and the observation data, the script and namelist file used in WRF-Chem and the scripts used for plotting, supporting the findings of this study. The release version of Python and the Scikit-Learn machine learning library are from https://scikit-learn.org/stable/index.html. The chemical compositions were adopted from Tsinghua University TAP (Tracking Air Pollution in China) dataset and available at http://tapdata.org.cn/?page_id=59&item=pm25 (last access: May, 2025, Geng et al., 2021). The meteorological datasets are from the fifth generation European Centre for Medium-Range Weather Forecasts reanalysis (ERA-5) and available at https://cds.climate.copernicus.eu/datasets (last access: May, 2025). The ground-based air quality monitoring observations are from the China National Environmental Monitoring Centre network and available from https://quotsoft.net/air/. The release version of WRF-Chem can be downloaded from http://www2.mmm.ucar.edu/wrf/users/download/get_source.html. The initial meteorological variables are from the National Center for Environmental Prediction's Final Operational Global (NCEP/FNL) and available from https://rda.ucar.edu/datasets/d083002/dataaccess/# (last access: May, 2025). The initial

https://doi.org/10.5194/egusphere-2025-1483
Preprint. Discussion started: 3 June 2025

and boundary chemical conditions are from the Community Atmosphere Model with Chemistry model and can be downloaded from (https://www.acom.ucar.edu/cam-chem/cam-chem.shtml last access: May, 2025). The anthropogenic emissions are from Multi resolution Emission Inventory for China (http://meicmodel.org.cn, last access: May, 2025, Zheng et al., 2018). The biological, biomass and fire emissions inventory are taken from the Model of Emissions of Gases and Aerosols from Nature and the Fire Inventory from NCAR, respectively (https://www.acom.ucar.edu/wrf-chem/download.shtml and https://www.acom.ucar.edu/Data/fire/ last access: May, 2025)

Supplement

The Supplement contains the information of the field campaigns, additional descriptions of the WRF-Chem simulation (study domain, emission inventory, parameterization scheme, and initial and boundary conditions), introductions of the auxiliary variables, and the method to evaluate aerosol indirect effects.

Author contributions

JYR: Conceptualization, Investigation, Formal analysis, Writing – original draft. SJZ: Data curation. HHX and GQL: Formal analysis. ZW: Formal analysis. ARZ: Data curation. CFZ: Technical support. MH: Data curation. DJS: Data curation. LZT: Data curation. RJH: Funding acquisition. YLS: Technical support. FZ: Writing-Reviewing and Editing, Funding acquisition. All authors read and approved the final manuscript.

https://doi.org/10.5194/egusphere-2025-1483
Preprint. Discussion started: 3 June 2025

Competing interests

The contact author has declared that none of the authors has any competing interests.

Acknowledgements

This work was funded by the National Natural Science Foundation of China (NSFC) research project (Grant No. 42405118, 42475112, 41975174), the State Key Laboratory of Loess and Quaternary Geology grant, the Institute of Earth Environment, Chinese Academy of Sciences (SKLLQG2429), Shenzhen Science and Technology Plan Project (Grant No. GXWD20220811174022002; KCXST20221021111404011), Guangdong Natural Science Foundation (Grant No. 2024A1515011005).

References

Albrecht, B.: Aerosols, cloud microphysics, and fractional cloudiness, Science, 245(4923), 1227 – 1230, https://doi.org/10.1126/science.245.4923.1227, 1989.

Charlson, R., Lovelock, J., Andreae, M., Warren, S.: Oceanic phytoplankton, atmospheric sulphur, cloud albedo and climate, Nature, 326(6114), 655 – 661, https://doi.org/10.1038/326655a0, 1987.

Chen, L., Zhang, F., Zhang, D. et al.: Measurement report: Hygroscopic growth of ambient fine particles measured at five sites in China, Atmos. Chem. Phys., 22(10), 6773 – 6786, https://doi.org/10.5194/acp-22-6773-2022, 2022.

Charlson, R. et al.: Climate Forcing by Anthropogenic Aerosols, Science, 255, 423 – 430, https://doi.org/ 10.1126/science.255.5043.423, 1992.

Fanourgakis, G., Kanakidou, M., Nenes, A. et al.: Evaluation of global simulations of aerosol particle and cloud condensation nuclei number, with implications for cloud droplet formation, Atmos. Chem. Phys., 19(13), 8591 – 8617, https://doi.org/ 10.5194/acp-19-8591-2019, 2019.

https://doi.org/10.5194/egusphere-2025-1483
Preprint. Discussion started: 3 June 2025

457 Fan, X., Liu, J., Zhang, F. et al.: Contrasting size-resolved hygroscopicity of fine
458 particles derived by HTDMA and HR-ToF-AMS measurements between summer
459 and winter in Beijing: the impacts of aerosol aging and local emissions, Atmos.
460 Chem. Phys., 20, 915 – 929, https://doi.org/10.5194/acp-20-915-2020, 2020.
461 Grange, S., Carslaw, D., Lewis, A. et al.: Random Forest meteorological normalisation
462 models for Swiss PM_{10} trend analysis, Atmos. Chem. Phys., 18(9), 6223 – 6239,
463 https://doi.org/10.5194/acp-18-6223-2018, 2018.
464 Geng, G., Xiao, Q., Liu, S. et al.: Tracking air pollution in China: near real-time PM2.
465 5 retrievals from multisource data fusion, Environmental Science & Technology,
466 55(17), 12106 – 12115, https://doi.org/10.1021/acs.est.1c01863, 2021.
467 Guo, J., Miao, Y., Zhang, Y. et al.: The climatology of planetary boundary layer height
468 in China derived from radiosonde and reanalysis data, Atmos. Chem. Phys., 16(20),
469 13309 – 13319, https://doi.org/10.5194/acp-16-13309-2016, 2016.
470 IPCC. Summary for Policymakers. In Climate Change 2021: The Physical Science
471 Basis. Contribution of Working Group I to the Sixth Assessment Report of the
472 Intergovernmental Panel on Climate Change; Cambridge University Press:
473 Cambridge, United Kingdom and New York, NY, USA. (2021).
474 Liu, C., Wang, T., Rosenfeld, D. et al.: Anthropogenic effects on cloud condensation
475 nuclei distribution and rain initiation in East Asia, Geophysical Research Letters,
476 47, https://doi.org/10.1029/2019GL086184, 2020.
477 Liu, J., Li, Z.: Significant underestimation in the optically based estimation of the
478 aerosol first indirect effect induced by the aerosol swelling effect, Geophysical
479 Research Letters, 45(11), 5690 – 5699, https://doi.org/10.1029/2018GL077679,
480 2018.
481 Liang, M., Tao, J., Ma, N. et al.: Prediction of CCN spectra parameters in the North
482 China Plain using a random forest model, Atmospheric Environment, 289, 119323,
483 https://doi.org/10.1016/j.atmosenv.2022.119323, 2022.

https://doi.org/10.5194/egusphere-2025-1483
Preprint. Discussion started: 3 June 2025

484 Li, S., Zhang, F., Jin, X. et al.: Characterizing the ratio of nitrate to sulfate in ambient
485 fine particles of urban Beijing during 2018-2019, Atmospheric Environment, 237,
486 https://doi.org/10.1016/j.atmosenv.2020.117662, 2020.
487 Liu, J., Zhang, F., Xu, W. et al.: Hygroscopicity of organic aerosols linked to formation
488 mechanisms, Geophysical Research Letters, 48,
489 https://doi.org/10.1029/2020GL091683, 2021.
490 Menon & Rotstayn.: The radiative influence of aerosol effects on liquid-phase cumulus
491 and stratiform clouds based on sensitivity studies with two climate models,
492 Climate Dynamics, 27, 4, 345 – 356, https://doi.org/10.1007/s00382-006-0139-3,
493 2006.
494 Moore, R., Cerully, K., Bahreini, R. et al.: Hygroscopicity and composition of
495 California CCN during summer 2010, Journal of Geophysical Research:
496 Atmospheres, 117, https://doi.org/10.1029/2011JD017352, 2012.
497 Morrison, H., Thompson, G., Tatarskii, V.: Impact of cloud microphysics on the
498 development of trailing stratiform precipitation in a simulated squall line:
499 Comparison of one-and two-moment schemes, Monthly Weather Review, 137(3),
500 991 – 1007, https://doi.org/10.1175/2008MWR2556.1, 2009.
501 Nair, A. A., Yu, F.: Using machine learning to derive cloud condensation nuclei number
502 concentrations from commonly available measurements, Atmos. Chem. Phys.,
503 20(21), 12853 – 12869, https://doi.org/10.5194/acp-20-12853-2020, 2020.
504 Nair, A. A., Yu, F., Campuzano-Jost, P. et al.: Machine learning uncovers aerosol size
505 information from chemistry and meteorology to quantify potential cloud-forming
506 particles, Geophysical Research Letters, 48, https://doi.org/
507 10.1029/2021GL094133, 2021.
508 Petters, M. D., Kreidenweis, S. M.: A single parameter representation of hygroscopic
509 growth and cloud condensation nucleus activity, Atmos. Chem. Phys., 7(8),
510 1961 – 1971, https://doi.org/10.5194/acp-7-1961-2007, 2007.
511 Ren, J., Zhang, F., Wang, Y. et al.: Using different assumptions of aerosol mixing state
512 and chemical composition to predict CCN concentrations based on field

https://doi.org/10.5194/egusphere-2025-1483
Preprint. Discussion started: 3 June 2025

measurements in urban Beijing, Atmos. Chem. Phys., 18(9), 6907 – 6921, https://doi.org/10.5194/acp-18-6907-2018, 2018.

Ren, J., Chen, L., Liu, J., and Zhang, F.: The density of ambient black carbon retrieved by a new method: implications for cloud condensation nuclei prediction, Atmos. Chem. Phys., 23, 4327 – 4342, https://doi.org/10.5194/acp-23-4327-2023, 2023.

Rose, C., Collaud Coen, M. et al.: Seasonality of the particle number concentration and size distribution: a global analysis retrieved from the network of Global Atmosphere Watch (GAW) near-surface observatories, Atmos. Chem. Phys., 21, 17185 – 17223, https://doi.org/10.5194/acp-21-17185-2021, 2021.

Rosenfeld, D., Zheng, Y., Hashimshoni, E. et al.: Satellite retrieval of cloud condensation nuclei concentrations by using clouds as CCN chambers, Proceedings of the National Academy of Sciences, 113(21), 5828 – 5834, https://doi.org/10.1073/pnas.1514044113, 2016.

Ren, J., Zou, S., Xu, H., Liu, G., Wang, Z., Zhang, A., Zhao, C., Hu, M., Shang, D., Tang, L., Huang, R.-J., Sun, Y., & Zhang, F.: Machine learning significantly improves the simulation of hourly-to-yearly scale cloud nuclei concentration and radiative forcing in polluted atmosphere [Data set]. Zenodo. https://zenodo.org/records/15523200, 2025.

Sotiropoulou, R. E. P., Nenes, A., Adams, P. J. et al.: Cloud condensation nuclei prediction error from application of Köhler theory: Importance for the aerosol indirect effect, Journal of Geophysical Research: Atmospheres, 112(D12) https://doi.org/10.1029/2006JD007834, 2007.

Shen, Y., Virkkula, A., Ding, A. et al.: Estimating cloud condensation nuclei number concentrations using aerosol optical properties: role of particle number size distribution and parameterization, Atmos. Chem. Phys., 19(24), 15483 – 15502, https://doi.org/10.5194/acp-19-15483-2019, 2019.

Sha, T., Ma, X.Y., Jia, H. L. et al.: Exploring the influence of two inventories on simulated air pollutants during winter over the Yangtze River Delta, Atmospheric

https://doi.org/10.5194/egusphere-2025-1483
Preprint. Discussion started: 3 June 2025

Environment, 206, 170 – 182, https://doi.org/10.1016/j.atmosenv.2019.03.006, 2019.

Schmale, J., Henning, S., Decesari, S. et al.: Long-term cloud condensation nuclei number concentration, particle number size distribution and chemical composition measurements at regionally representative observatories, Atmos. Chem. Phys., 18(4), 2853 – 2881, https://doi.org/10.5194/acp-18-2853-2018, 2018.

Song, C., Becagli, S., Beddows, D. C. S. et al.: Understanding Sources and Drivers of Size-Resolved Aerosol in the High Arctic Islands of Svalbard Using a Receptor Model Coupled with Machine Learning, Environmental Science & Technology, 56(16), 11189 – 11198, https://doi.org/10.1021/acs.est.1c07796, 2022.

Shang, D., Tang, L., Fang, X. et al.: Variations in source contributions of particle number concentration under long-term emission control in winter of urban Beijing, Environmental Pollution, 304, 119072, https://doi.org/10.1016/j.envpol.2022.119072, 2022.

Stier, P., van, den, Heever, S, C., Christensen, M. W. et al.: Multifaceted aerosol effects on precipitation, Nature Geoscience, 17(8), 719 – 732, https://doi.org/10.1038/s41561-024-01482-6, 2024.

Twomey, S.: The influence of pollution on the shortwave albedo of clouds, Journal of the atmospheric sciences, 34(7), 1149-1152, https://doi.org/10.1175/1520-0469(1977)034<1149:TIOPOT>2.0.CO;2, 1977.

Wei, J., Li, Z., Wang, J. et al.: Ground-level gaseous pollutants (NO_2, SO_2, and CO) in China: daily seamless mapping and spatiotemporal variations, Atmos. Chem. Phys., 23, 1511 – 1532, https://doi.org/10.5194/acp-23-1511-2023, 2023.

Wang, Y., Niu, S., Lv, J. et al.: A new method for distinguishing unactivated particles in cloud condensation nuclei measurements: implications for aerosol indirect effect evaluation, Geophysical Research Letters, 46, 14,185 – 14,194, https://doi.org/10.1029/2019GL085379, 2019.

Wang, J., Lee, Y.-N., Daum, P. H., Jayne, J., and Alexander, M. L.: Effects of aerosol organics on cloud condensation nucleus (CCN) concentration and first indirect

https://doi.org/10.5194/egusphere-2025-1483
Preprint. Discussion started: 3 June 2025

aerosol effect, Atmos. Chem. Phys., 8, 6325 – 6339, https://doi.org/10.5194/acp-8-6325-2008, 2008.

Xu, W., Fossum, K. N., Ovadnevaite, J. et al.: The impact of aerosol size-dependent hygroscopicity and mixing state on the cloud condensation nuclei potential over the north-east Atlantic, Atmos. Chem. Phys., 21, 8655 – 8675, https://doi.org/10.5194/acp-21-8655-2021, 2021.

Yang, N., Shi, H., Tang, H. et al.: Geographical and temporal encoding for improving the estimation of $PM_{2.5}$ concentrations in China using end-to-end gradient boosting, Remote Sensing of Environment, 269, 112828, https://doi.org/10.1016/j.rse.2021.112828, 2022.

Yu, F., Luo, G., Nair, A. A., Tsigaridis, K., & Bauer, S. E.: Use of machine learning to reduce uncertainties in particle number concentration and aerosol indirect radiative forcing predicted by climate models, Geophysical Research Letters, 49, https://doi.org/10.1029/2022GL098551, 2022.

Yu, F., Luo, G., Nair, A. A. et al.: Wintertime new particle formation and its contribution to cloud condensation nuclei in the Northeastern United States, Atmos. Chem. Phys., 20(4), 2591 – 2601, https://doi.org/10.5194/acp-20-2591-2020, 2020.

Zhu, Y., Shen, Y., Li, K. et al.: Investigation of particle number concentrations and new particle formation with largely reduced air pollutant emissions at a coastal semi-urban site in northern China, Journal of Geophysical Research: Atmospheres, 126, e2021JD035419, https://doi.org/10.1029/2021JD035419, 2021.

Zhang, F., Li, Y., Li, Z. et al.: Aerosol hygroscopicity and cloud condensation nuclei activity during the AC3Exp campaign: Implications for cloud condensation nuclei parameterization, Atmos. Chem. Phys., 14(24), 13423–13437, https://doi.org/10.5194/acp-14-13423-2014, 2014.

Zhang, F., Li, Z., Li, Y. et al.: Impacts of organic aerosols and its oxidation level on CCN activity from measurement at a suburban site in China, Atmos. Chem. Phys., 16(8), 5413 – 5425, https://doi.org/10.5194/acp-16-5413-2016, 2016.

https://doi.org/10.5194/egusphere-2025-1483
Preprint. Discussion started: 3 June 2025

598 Zhang, F., Ren, J., Fan, T. et al.: Significantly enhanced aerosol CCN activity and
599 number concentrations by nucleation-initiated haze events: A case study in urban
600 Beijing, Journal of Geophysical Research: Atmospheres, 124(24), 14102 – 14113,
601 https://doi.org/10.1029/2019JD031457, 2019.
602 Zhang, F., Wang, Y., Peng, J. et al.: Uncertainty in predicting CCN activity of aged and
603 primary aerosols, Journal of Geophysical Research: Atmospheres, 122(21),
604 11723 – 11736, https://doi.org/10.1002/2017JD027058, 2017.
605 Zaveri, R. A., Peters, L. K.: A new lumped structure photochemical mechanism for
606 large-scale applications, Journal of Geophysical Research: Atmospheres, 104,
607 30387 – 30415, https://doi.org/10.1029/1999JD900876, 1999.
608 Zheng, B., Tong, D., Li, M., Liu, F. et al.: Trends in China's anthropogenic emissions
609 since 2010 as the consequence of clean air actions, Atmos. Chem. Phys., 18,
610 14095-14111, https://doi.org/10.5194/acp-18-14095-2018, 2018.

611 ## Figures

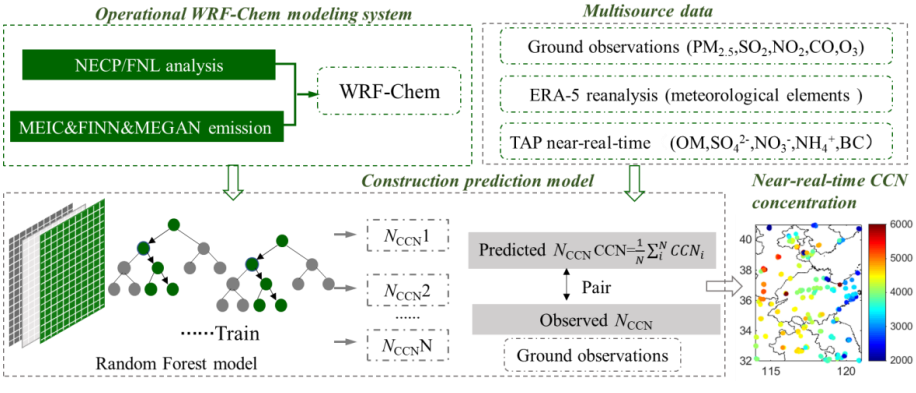

612

613 **Fig. 1** Methodological framework of CCN number concentration prediction.

https://doi.org/10.5194/egusphere-2025-1483
Preprint. Discussion started: 3 June 2025

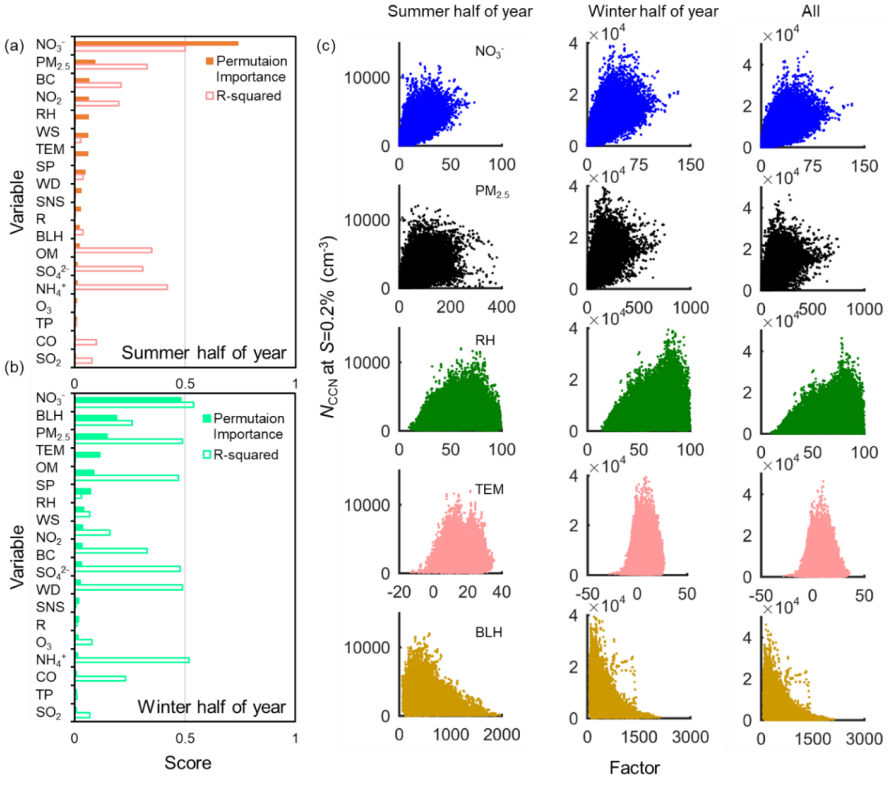

Fig. 2 The relative importance of the input parameters to the prediction of N_{CCN}. (a) Permutation importance of each parameter and its determination coefficient in the summer half of year; (b) Same as (a) but for the winter half of year; (c) Scatter plots of the input parameters (NO_3^-, $PM_{2.5}$, RH, TEM, BLH) with CCN number concentration at S=0.2%.

https://doi.org/10.5194/egusphere-2025-1483
Preprint. Discussion started: 3 June 2025

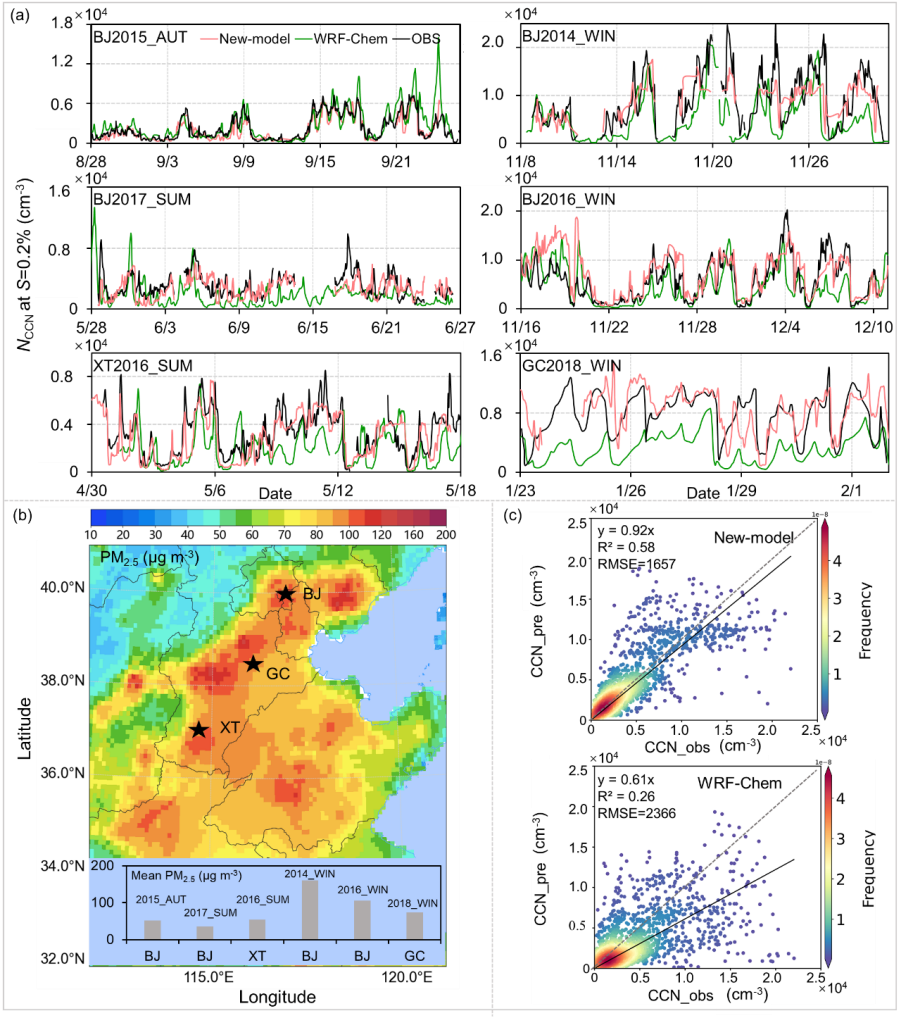

620 **Fig. 3** Performance of the new model in predicting N_{CCN} at field sites in NCP. (a) Time
621 series of the observed and predicted CCN number concentrations at S=0.2% for the six
622 campaigns (BJ2015_AUT, BJ2017_SUM, XT2016_SUM, BJ2014_WIN,
623 BJ2016_WIN, GC2018_WIN) in the North China Plain; (b) Map for average mass
624 concentration of $PM_{2.5}$ of 2014 from TAP dataset in NCP (http://tapdata.org.cn/) and
625 field observed average mass concentration of $PM_{2.5}$ during the six field campaigns (see

https://doi.org/10.5194/egusphere-2025-1483
Preprint. Discussion started: 3 June 2025

626 embedded histogram); (c) Scatter plots of the observed N_{CCN} at S=0.2% with the New-
627 model predicted (top) and WRF-Chem simulated (bottom) respectively.

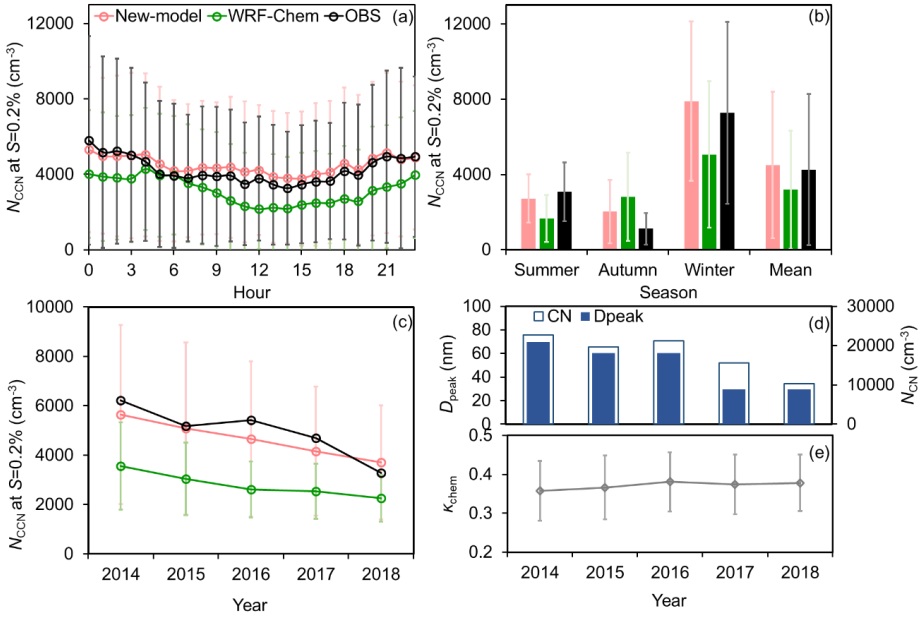

628

629 **Fig. 4** Performance of the new model in predicting hourly-to-yearly scale N_{CCN}. (a)
630 Diurnal variations of N_{CCN} at S=0.2% derived from the new model, the WRF-Chem,
631 and the observations from the field campaigns; (b) Seasonal variations, here the
632 comparison in summer, autumn and winter were conducted using the campaign
633 averages of BJ2017_SUM, BJ2015_AUT, and BJ2014_WIN&BJ2016_WIN
634 respectively with the new model and WRF-Chem predictions at corresponding periods;
635 (c) Trends of annual mean N_{CCN} from 2014 to 2018; (d) Trends of annual mean particle
636 number concentration and peak diameter; (e) Trends of annual mean of the hygroscopic
637 parameter κ_{chem} calculated from TAP dataset in Beijing.

https://doi.org/10.5194/egusphere-2025-1483
Preprint. Discussion started: 3 June 2025

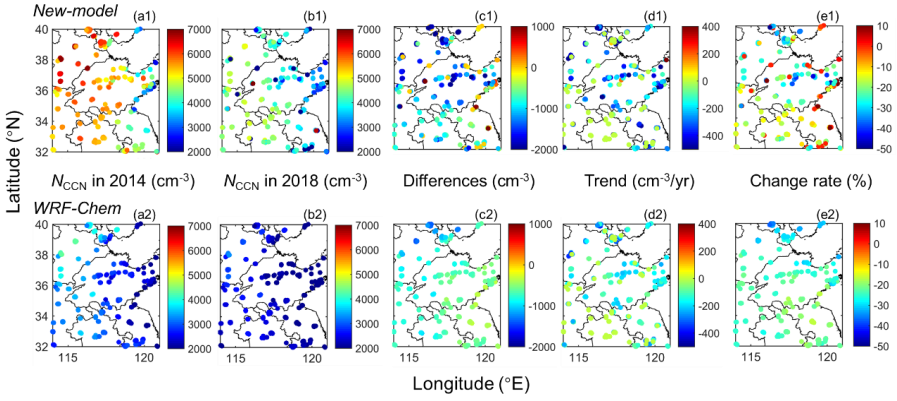

Fig. 5 Spatial variations of N_{CCN} derived by the new model (top) and WRF-Chem (bottom) at the sites in the studied region. (a1) Average N_{CCN} at S=0.2% in 2014 predicted by the new model; (a2) Average N_{CCN} at S=0.2% in 2014 by the WRF-Chem; (b1 and b2) Same as a1 and a2 but in 2018; (c1) Differences in N_{CCN} at S=0.2% between the year of 2014 and 2018 predicted by the new model; (c2) Same as (c1) but by the WRF-Chem; (d1) Trends of N_{CCN} at S=0.2% from 2014 to 2018 predicted by the new model ; (d2) Same as (d1) but by the WRF-Chem; (e1) Change rates of N_{CCN} at S=0.2% from 2014 to 2018 predicted by the new model; (e2) Same as (e1) but by the WRF-Chem.

https://doi.org/10.5194/egusphere-2025-1483
Preprint. Discussion started: 3 June 2025

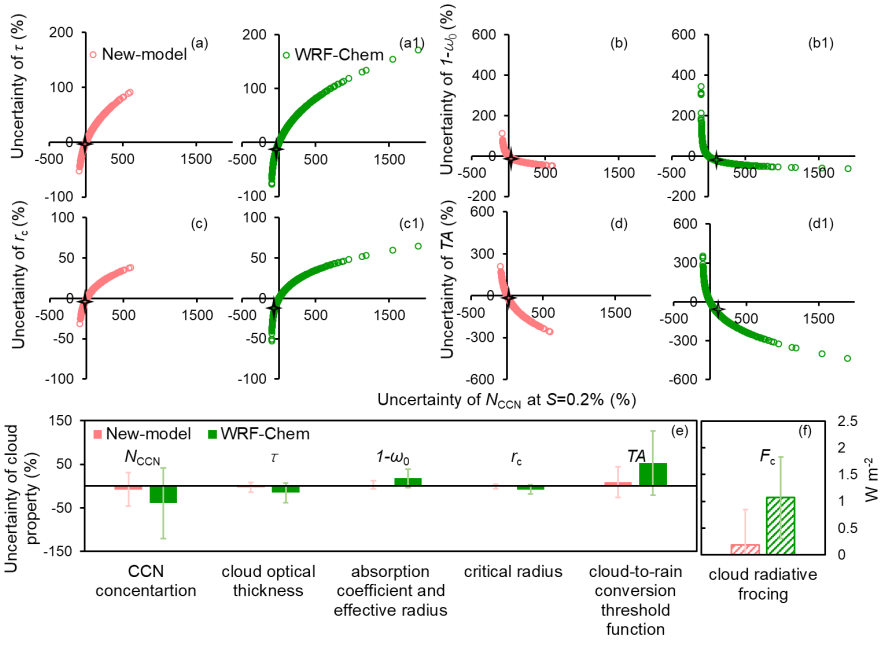

Fig. 6 Sensitivity of the cloud parameters and radiative forcing to CCN prediction biases. (a) Dependence of the uncertainty of the cloud optical thickness (τ) on the uncertainty of N_{CCN} at S=0.2% with the new model; (a1) Same as (a) but by the WRF-Chem; (b) Dependence of the uncertainty of the absorption coefficient (1-ω_0) on the uncertainty of N_{CCN} at S=0.2% with the new model; (b1) Same as (b) but by the by the WRF-Chem; (c) Dependence of the uncertainty of the critical radius (r_c) on the uncertainty of N_{CCN} at S=0.2% with the new model; (c1) Same as (c) but by the WRF-Chem; (d) Dependence of the uncertainty of the cloud-to-rain conversion threshold function (TA) on the uncertainty of N_{CCN} at S=0.2% with the new model; (d1) Same as (d) but by the WRF-Chem; (e) Mean uncertainty in simulating the cloud properties and (f) radiative forcing (F_c) by the new model and the WRF-Chem; Black star shows the mean value for the observation.